

Exact solution for the degenerate ground-state manifold of a strongly interacting one-dimensional Bose-Fermi mixture

Bess Fang,^{1,2} Patrizia Vignolo,³ Mario Gattobigio,³ Christian Miniatura,^{1,2,3} and Anna Minguzzi⁴

¹*Department of Physics, Block S12, Faculty of Science,*

National University of Singapore, 2 Science Drive 3, Singapore 117542

²*Centre for Quantum Technologies, National University of Singapore, 3 Science Drive 2, Singapore 117543*

³*Université de Nice-Sophia Antipolis, Institut Non Linéaire de Nice,*

CNRS; 1361 route des Lucioles, 06560 Valbonne, France

⁴*Université Grenoble 1, CNRS, LPMMC, UMR5493, Maison des Magistères, 38042 Grenoble, France*

(Dated: November 7, 2018)

We present the exact solution for the many-body wavefunction of a one-dimensional mixture of bosons and spin-polarized fermions with equal masses and infinitely strong repulsive interactions under external confinement. Such a model displays a large degeneracy of the ground state. Using a generalized Bose-Fermi mapping we find the solution for the whole set of ground-state wavefunctions of the degenerate manifold and we characterize them according to group-symmetry considerations. We find that the density profile and the momentum distribution depends on the symmetry of the solution. By combining the wavefunctions of the degenerate manifold with suitable symmetry and guided by the strong-coupling form of the Bethe-Ansatz solution for the homogeneous system we propose an analytic expression for the many-body wavefunction of the inhomogeneous system which well describes the ground state at finite, large and equal interactions strengths, as validated by numerical simulations.

PACS numbers: 05.30.-d,67.85.-d,67.85.Pq

I. INTRODUCTION

Ultracold atomic gases provide a versatile and controlled system for the study of quantum correlations and fluctuations which are particularly strong in one dimension (1D). Experiments on two-dimensional optical lattices [1–4] or on a chip trap [5] have reached the strongly interacting Tonks-Girardeau regime. In such impenetrable boson limit, repulsive interactions play the role of the Pauli exclusion principle and the many-body wavefunction can be exactly obtained by mapping onto the one of noninteracting fermions [6]. Experimental advances on trapping and cooling ultracold Bose-Fermi mixtures [7–12] and the possibility of trapping both species in tight atomic waveguides have boosted a theoretical activity on 1D mixtures. At increasing boson-fermion repulsions, mean-field [13] and Luttinger liquid analysis at weak coupling [14] predict an instability towards phase separation (i.e. demixing) of the two components. For a highly symmetric model with equal masses and coupling constants, further progress can be made by use of exact solutions. For the homogeneous system, a Bethe-Ansatz solution is known [15–17] and no demixing is found. The long-wavelength properties of its correlation functions have been studied using conformal field theory [18]. Inhomogeneous systems, as in the case of experiments, bring about novel issues, such as the spatial structure of the ground state. At intermediate interaction strength a partial demixing of the two clouds has been found by a local density approximation on the Bethe-Ansatz solution both at zero and finite temperature [17, 19, 20]. In the Tonks-Girardeau limit of infinitely strong boson-boson and boson-fermion repulsions a large ground state

degeneracy is expected [21], and is associated to the freedom of fixing the sign of the many-body wavefunction under the exchange of a boson with a fermion. For an inhomogeneous system, one exact solution of the degenerate manifold has been proposed in [21] and analyzed in detail in [22–24]. The corresponding density profiles display no demixing among the two species. Till now no expression was known for the other wavefunctions of the manifold. In this work we solve several open theoretical issues. First of all we find an exact analytical solution for all the wavefunctions of the degenerate manifold in the Tonks-Girardeau limit, thus generalizing the solution of [21]. Secondly, we characterize the solutions in terms of their symmetry properties according to group theory considerations. At difference from fermionic or bosonic spinor systems [25, 26], where the state of the system can be labelled on the basis of the spin quantum number, in order to label the states of the Bose-Fermi mixture we introduce a suitable Casimir operator which reflects the mixed symmetry under particle exchange. Furthermore, we find that such symmetry considerations allow for the understanding of the shape of the momentum distribution, which depends on the choice of the wavefunction within the manifold. Finally, by linear combination of the basis wavefunctions of the degenerate manifold we individuate the wavefunction which corresponds to the ground state at finite, large and equal interactions strengths, and we confirm this prediction by comparing with numerical DMRG simulations. For the nontrivial case of the Bose-Fermi mixture with large degeneracy, this analysis allows for the first time to draw a link between the Bethe-Ansatz solution of the homogeneous system and the Tonks-Girardeau solution of the inhomoge-

neous system. Our solution sheds light onto the general properties of the ground state wavefunction of a fully quantum problem in the strongly interacting limit.

II. ORTHONORMAL BASIS SET FOR THE DEGENERATE GROUND-STATE MANIFOLD

A. General considerations

We consider the model of N_B bosons and N_F spin-polarized fermions of masses $m_B = m_F = m$, confined by the same external potential. The particles interact via the contact potentials, $v_{BB}(x) = g_{BB}\delta(x)$, $v_{BF}(x) = g_{BF}\delta(x)$, and we focus on the limit $g_{BB} = g_{BF} \rightarrow \infty$. The effect of contact interactions can be replaced by the boundary condition that the wavefunction vanishes at each BB or BF contact, i.e.

$$\Psi(\dots, x_j, \dots, x_\ell, \dots) = 0 \text{ whenever } x_j = x_\ell. \quad (1)$$

We adopt the convention that $\{x_1, \dots, x_{N_B}\}$ are bosonic coordinates and $\{x_{N_B+1}, \dots, x_N\}$ are fermionic ones. The ground state has a large degeneracy $C_{N_B}^N = N!/N_B!/N_F!$, which can be interpreted as choosing N_B positions for the bosons out of $N = N_B + N_F$, and amounts to fixing in several possible ways the sign of the wavefunction under the exchange of bosons with fermions.

In order to determine an orthonormal basis set for the degenerate manifold we proceed as follows. Consider a fermionic Slater determinant made of the first *total* N orbitals,

$$\Psi_F(x_1, \dots, x_N) = \frac{1}{\sqrt{N!}} \det[\phi_j(x_\ell)], \quad (2)$$

where $j, \ell = 1, \dots, N$, and $\phi_j(x)$ are obtained by the solution of the single-particle Schroedinger equation in the potential $V(x)$. Ψ_F displays the correct nodes at each *BB* and *BF* contact. In a given coordinate sector, $x_{P(1)} < x_{P(2)} < \dots < x_{P(N)}$, with P being a permutation among the N particles, the required many-body wavefunction is proportional to $\Psi_F(x_1, \dots, x_N)$. A useful set of orthonormal basis is given by the “snippets” [25]

$$\langle x_1, \dots, x_N | P \rangle = \sqrt{N!} |\Psi_F(x_1, \dots, x_N)| \quad (3)$$

in the coordinate sector $x_{P(1)} < x_{P(2)} < \dots < x_{P(N)}$, and zero otherwise. To build the required basis for the manifold, we now collect the snippets which correspond to exchanging only the positions of the bosons or of the fermions *among themselves*, using the Fermi or Bose statistics to fix the relative sign of the various terms. The number of groups of snippets subdivided in such a way is exactly $C_{N_B}^N$. This yields the required orthonormal basis set $\{\Psi^\alpha\}$ for the degenerate manifold, since each snippet is orthogonal to another and is used only once.

The density profiles associated to each wavefunction Ψ_α are given by

$$n_B^\alpha(x) = N_B \int dx_2 \dots dx_N |\Psi_\alpha(x, x_2 \dots x_N)|^2, \\ n_F^\alpha(x) = N_F \int dx_1 \dots dx_{N-1} |\Psi_\alpha(x_1, \dots, x_{N-1}, x)|^2, \quad (4)$$

which is equivalent to computing

$$n_{B(F)}^\alpha(x) = \sum_{i=1}^N p_{i,B(F)}^\alpha \rho_i(x), \quad (5)$$

with $p_{i,B(F)}^\alpha = 1$ if a boson (fermion) is at position $i = 1, \dots, N$ in the configuration α and zero otherwise, and

$$\rho_i(x) = \int_{x_1 < x_2 < \dots < x_N} dx_1 \dots dx_N |\Psi_F(x_1, \dots, x_N)|^2 \delta(x - x_i). \quad (6)$$

B. An illustration with $N_B = N_F = 2$

We illustrate the idea in the case $N = 4$, $N_B = N_F = 2$, and take a harmonic confinement $V(x) = \frac{1}{2}m\omega^2 x^2$ for simplicity, assuming the same trapping frequency ω for the two species. We denote the bosonic coordinates by x_1, x_2 and the fermionic ones by x_3, x_4 , and we expect a six-fold degeneracy. We label the basis set using the positions of the particles, i.e. BBFF, BFBF, BFFB, FBBF, FBFB, FFBB. Let us call this basis the “BBFF” basis. According to the above prescription the first wavefunction is

$$\Psi_{BBFF} = \frac{1}{2} [(x_1, x_2, x_3, x_4 | (e + (12))(e - (34)))] , \quad (7)$$

where by $(j\ell)$ we denote the permutation between the particles j and ℓ , e is the identity permutation, and we adopt the usual convention of product among permutations [27]; the snippet basis satisfies $\langle x_1, \dots, x_N | P + Q \rangle = \langle x_1, \dots, x_N | P \rangle + \langle x_1, \dots, x_N | Q \rangle$. Similarly, the second wavefunction is obtained by

$$\Psi_{BFBF} = \frac{1}{2} [(x_1, x_3, x_2, x_4 | (e + (12))(e - (34)))] . \quad (8)$$

The other wavefunctions are built in the same way, taking as initial coordinate sector the one where the bosonic and fermionic coordinates are each in ascending order.

We display the density profiles of the six basis states in Fig.1. Each peak corresponds to the position of a particle in the BBFF sequence, hence the basis set recalls the one of distinguishable particles, as in the case of spinor bosons [25].

III. SYMMETRY CHARACTERIZATION

A. Casimir invariance of the manifold

We would like to label the basis vectors by some additional quantum number. We proceed by exploiting the

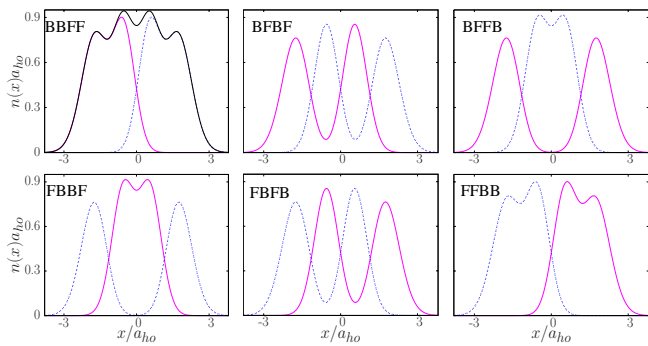


FIG. 1. (Color online) Bosonic (magenta solid line) and fermionic (blue dashed line) density profiles (in units of $a_{ho}^{-1} = \sqrt{m\omega/\hbar}$) as a function of the spatial coordinate x (in units of a_{ho}) for each BBFF wavefunction of the $N_B = N_F = 2$ mixture. The total density (black solid thin line) is included in the first frame for reference.

exchange symmetry between bosons or fermions among themselves. According to a group theoretical analysis, there are only two possible Young tableaux associated to a quantum mechanical system of mixed Bose-Fermi symmetry, i.e. symmetric in its first N_B coordinates and antisymmetric in its last N_F :

$$Y = \begin{array}{|c|c|c|c|} \hline F_1 & B_1 & \cdots & B_{N_B} \\ \hline \vdots & & & \\ \hline F_{N_F} & & & \\ \hline \end{array}, \quad Y' = \begin{array}{|c|c|} \hline B_1 & \cdots B_{N_B} \\ \hline F_1 \\ \hline \vdots \\ \hline F_{N_F} \\ \hline \end{array}, \quad (9)$$

each with a dimension of $C_{N_B}^{N-1}$, $C_{N_F}^{N-1}$ respectively.

To each Young tableau it is possible to associate a value of a Casimir invariant, obtained from the generators of the permutation group \mathcal{S}_N , and which commutes with all elements of the group. In this particular case we choose $\mathcal{C} = \sum_{i < j} (ij)$, the sum over all the transpositions [28]. Two different eigenvalues of the Casimir operator are associated to the two tableaux, namely

$$\begin{aligned} \mathcal{C}_Y &= C_2^{N_B+1} - C_2^{N_F-1}, \\ \mathcal{C}_{Y'} &= C_2^{N_B-1} - C_2^{N_F+1}, \end{aligned} \quad (10)$$

with degeneracy corresponding to the dimension of the tableau. We remark that the eigenvalue $\mathcal{C}_{Y(Y')}$ essentially counts the number of two-particle exchange allowed by the corresponding tableau, where a symmetric permutation (from the row) is counted as +1 and an antisymmetric permutation (from the column) is counted as -1.

We represent the Casimir operator on the BBFF orthonormal basis set (see appendix A for some examples). The eigenvectors of the Casimir operators, obtained by diagonalization, are expressed as linear combinations of the BBFF basis vectors, and provide an alternative (but not orthonormal) basis set $\Psi_\mu(x_1, \dots, x_N)$ characterized by the symmetry of the tableau.

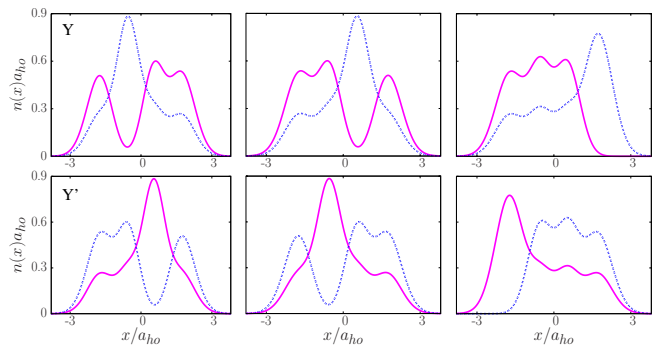


FIG. 2. (Color online) Bosonic (magenta solid line) and fermionic (blue dashed line) density profiles (in units of a_{ho}^{-1}) as a function of the spatial coordinate x (in units of a_{ho}) with the Y (top) and Y' (bottom) symmetry for $N_B = N_F = 2$.

The related bosonic and fermionic momentum distributions

$$n_{B(F)}^\mu(p) = \frac{1}{2\pi} \int dx dx' e^{-ip(x-x')} \rho_{B(F)}^\mu(x, x') \quad (11)$$

can be computed from the bosonic and fermionic one-body density matrix

$$\begin{aligned} \rho_B^\mu(x, x') &= N_B \int dx_2 \dots dx_N \Psi_\mu^*(x, x_2, \dots, x_N) \\ &\quad \times \Psi_\mu(x', x_2, \dots, x_N), \\ \rho_F^\mu(x, x') &= N_F \int dx_1 \dots dx_{N-1} \Psi_\mu^*(x_1, \dots, x_{N-1}, x) \\ &\quad \times \Psi_\mu(x_1, \dots, x_{N-1}, x'). \end{aligned} \quad (12)$$

B. Density profiles and momentum distributions at a given symmetry

We return to the earlier example of two bosons and two fermions in a harmonic confinement. The density profiles of the eigenstates of Y and Y' are shown in Fig. 2. We notice that in this highly symmetric problem the role of bosons and fermions is simply exchanged among the two submanifolds.

We also display the corresponding momentum distributions in Fig.3. It is worth mentioning that the momentum distributions associated to the Y symmetry display less peaks (with a number of peaks in $n_F(p)$ equal to N_F as in [22]) and are narrower than those associated to the Y' symmetry, following the intuition that the symmetry of the latter tableau is more ‘‘Fermi-like’’ (i.e. extended in the vertical direction).

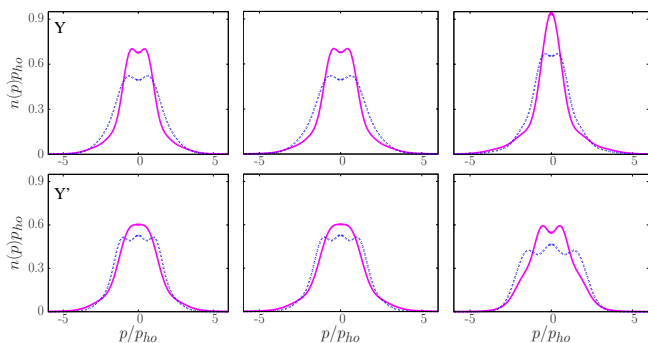


FIG. 3. (Color online) Bosonic (magenta solid line) and fermionic (blue dashed line) momentum distributions (in units of $p_{ho}^{-1} = 1/\sqrt{\hbar m \omega}$) as a function of p (in units of p_{ho}) with the Y (top) and Y' (bottom) symmetry for $N_B = N_F = 2$. The first and second panels in each row coincide.

IV. GROUND STATE AT LARGE, FINITE INTERACTION STRENGTH

A. Analysis of special solutions

At finite interactions $g_{BB} = g_{BF}$, the ground state is expected to display the Y symmetry [15, 29], since the associated wavefunction has less nodes than the one with Y' symmetry. From a continuity argument starting from the noninteracting solution, we also expect that it is nonvanishing in all permutation sectors. In Ref.[21] a special solution with the latter property was proposed,

$$\Psi_{GM} = A_{BB} A_{BF} \Psi_F(x_1, \dots, x_N), \quad (13)$$

where the mapping functions are

$$\begin{aligned} A_{BB} &= \prod_{1 \leq j < \ell \leq N_B} \text{sgn}(x_j - x_\ell), \\ A_{BF} &= \prod_{1 \leq j \leq N_B, N_B+1 \leq \ell \leq N} \text{sgn}(x_j - x_\ell). \end{aligned} \quad (14)$$

We test its symmetry by evaluating the average value of the Casimir operator $\langle \mathcal{C} \rangle = \langle \Psi | \mathcal{C} | \Psi \rangle / \langle \Psi | \Psi \rangle$. The expression of the (unnormalized) GM wavefunction on the BBFF basis $\Psi_{GM} = \sum_{\alpha=1}^{N!/N_F!/N_B!} c_\alpha \Psi_\alpha$ is $c_\alpha = 1$ for any α . From the representation of the Casimir operator (see appendix A) we obtain that for $N_B = N_F = 3$ the average value of the Casimir operator corresponds to its maximal eigenvalue $\mathcal{C}_Y = 3$, hence the GM wavefunction has the symmetry of the Y tableau. This is not the case for $N_B = N_F = 2$ where a wavefunction which is nonvanishing in all coordinate sectors and has the Y symmetry is $\Psi'_{GM} = A_{BB} \Psi_F(x_1, \dots, x_N)$. More generally, we have proven that the GM wavefunction with odd $N_B = N_F$ has always the symmetry of the Y tableau (see appendix B for demonstration).

For the homogeneous system, the Bethe-Ansatz method provides a solution of the model of a Bose-Fermi mixture with equal bosonic and fermionic masses and finite but equal coupling strengths $g_{BB} = g_{BF}$ [15, 17, 19]. The solution for the many-body wavefunction is built

with the symmetry of a given tableau [30, 31]. In analogy with fermionic systems, the solution is expressed in terms of spatial coordinates and “pseudospin” integer coordinates y_i which correspond to the relative positions of the bosons in the coordinate sector $x_{P(1)} < x_{P(2)} < \dots < x_{P(N)}$, namely $\{y_1, \dots, y_{N_B}\} = \{P^{-1}(1), \dots, P^{-1}(N_B)\}$. In Ref.[19] Imambekov and Demler study the strongly interacting limit of the Bethe-Ansatz solution (BA) for N_B, N_F odd. They notice that the wavefunction decouples as a product of an “orbital” part and a “spin” part, as

$$\Psi_{BA} \sim \det[e^{i\frac{2\pi}{N}\kappa_i y_j}] \Psi_F(x_1, \dots, x_N), \quad (15)$$

where the orbital part is a Slater determinant of the first N orbitals, of course chosen for the homogeneous problem $\Psi_F(x_1, \dots, x_N) = (1/\sqrt{N!}) \det[e^{ik_j x_\ell}]$, and the “spin” part includes only the bosonic coordinates y_1, \dots, y_{N_B} , with $\kappa = \{-(N_B - 1)/2 + N/2, \dots, N/2, \dots, (N_B - 1)/2 + N/2\}$ for the ground state. Taking advantage of the decoupling among orbital and spin part of the wavefunction, we generalize such a solution to the inhomogeneous system, by replacing the orbital part of (15) by its corresponding expression under confinement, Eq. (2). We check its symmetry by evaluating the average of the Casimir operator. For $N_B = N_F = 3$ an explicit calculation by expansion of (15) on the BBFF basis yields the maximal value $\langle \Psi_{BA} | \mathcal{C} | \Psi_{BA} \rangle / \langle \Psi_{BA} | \Psi_{BA} \rangle = 3$, implying that the generalized BA wavefunction has the Y symmetry. By construction, the BA solution for the trapped case has the same form as the one obtained for arbitrary interactions in the homogeneous system [34]. Notice that although the GM and generalized BA wavefunctions are not simply proportional to each other, their density profiles coincide, displaying no demixing. We remark that Eq. (15) can generate a wavefunction with the Y' symmetry by adopting a different choice of spin rapidities, e.g. for $\kappa = \{-(N_B - 1)/2, \dots, 0, \dots, (N_B - 1)/2\}$ we obtain an average Casimir operator equal to -3 .

It is important to notice that the form of the solution for the wavefunction at finite large interactions depends from the way in which the limit $g_{BB} \rightarrow \infty$ and $g_{BF} \rightarrow \infty$ is approached. Consider for example the case where g_{BB} tends to infinity and g_{BF} is finite. The above symmetry classifications are not useful in this case. The bosonic component can be mapped onto a fermionic one, and the problem can be reduced to the one of spin 1/2 fermions as in [35]. Also in such a case a decoupling of spatial and spin degrees of freedom is predicted with a different form for the spin part with respect to Eq.(15).

B. Numerical illustration

We have tested our predictions by comparing with numerical DMRG simulations [36]. The DMRG techniques provides an efficient numerical solution for the lattice model of an interacting Bose-Fermi mixture subjected

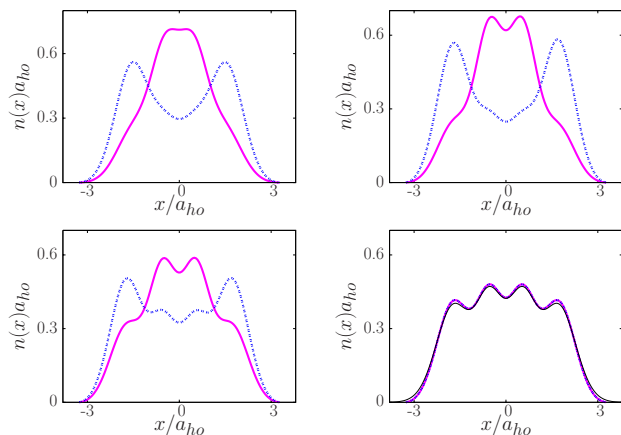


FIG. 4. (Color online) Bosonic (magenta solid line) and fermionic (blue dashed line) density profiles as obtained from DMRG simulations (in units of a_{ho}^{-1}) as a function of x (in units of a_{ho}) at increasing interaction strength $U/t = 1, 10, 10^2, 10^4$ (from left to right and from top to bottom). The harmonic trap strength is $V/t = 7 \times 10^{-6}$ and the number of lattice sites used in the simulation is $L = 128$. In the last panel the analytical prediction from the generalized BA wavefunction (thin black solid line) is shown.

to an external potential, described by the Hamiltonian

$$\begin{aligned} \mathcal{H} = & -t \sum_j (b_j^\dagger b_{j+1} + h.c.) - t \sum_j (f_j^\dagger f_{j+1} + h.c.) \\ & + U_{BB} \sum_j n_{B,j} (n_{B,j} - 1) + U_{BF} \sum_j n_{B,j} n_{F,j} \\ & + \sum_j V (j - L/2)^2 (n_{B,j} + n_{F,j}). \end{aligned} \quad (16)$$

Here, b_j and f_j are the bosonic and fermionic field operators acting on a site j , with corresponding density operators $n_{B,j} = b_j^\dagger b_j$ and $n_{F,j} = f_j^\dagger f_j$, t is the tunnel constant, U_{BB} and U_{BF} are the on-site BB and BF interactions, V is the strength of the external harmonic confinement, which is taken to be the same for bosons and fermions, and L is the number of sites in the lattice.

Since in the limit of very low lattice filling the lattice model reproduces the continuum model, we have used this method to obtain the ground-state density profiles and momentum distributions for the Bose-Fermi mixture at increasing interaction strength. For the sake of comparing with the previously proposed special solutions we have restricted ourselves to the case of equal BB and BF interactions, $U \equiv U_{BB} = U_{BF}$. Figure 4 displays the bosonic and fermionic density profiles for a Bose-Fermi mixture with $N_B = 2$, $N_F = 2$ at increasing interaction strength. The density profiles evolve from a partially demixed one at intermediate interaction strength, to a nondemixed one at large interactions, in agreement with the predictions of the GM and generalized BA wavefunctions. This behaviour was also noticed in a density functional calculation [32]. For a Bose-Bose mixture a similar absence of demixing at strong coupling was observed [33].

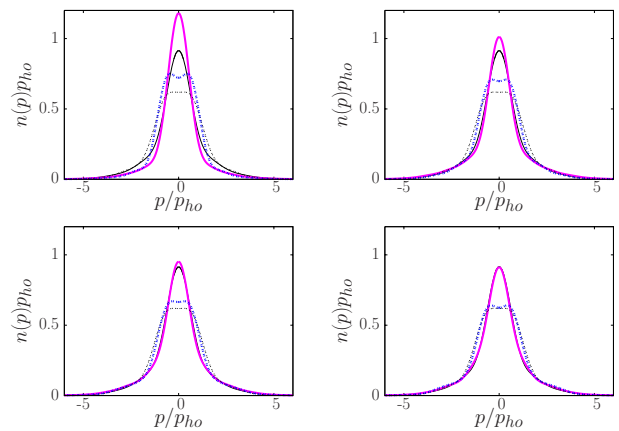


FIG. 5. (Color online) Bosonic (magenta solid lines) and fermionic (blue dashed lines) momentum distributions (in units of $p_{ho}^{-1} = 1/\sqrt{\hbar m \omega}$) as a function of p (in units of p_{ho}), from the numerical DMRG data at increasing interaction strength ($U/t = 1, 10, 10^2, 10^4$, from top to bottom and from left to right, thick lines). At increasing interactions the curves approach the analytical predictions from the generalized BA wavefunction for the bosonic (thin black solid lines) and fermionic (thin black dashed lines) momentum distributions, shown in each panel for reference (almost indistinguishable from the numerical data in the last panel). The other parameters used in the simulation are $V/t = 7 \times 10^{-6}$ and $L = 128$.

The momentum distributions for the bosonic and fermionic components are illustrated in Fig.5 as compared with the predictions of the generalized BA wavefunction. At increasing the interaction strength the momentum distributions approach those obtained by the generalized BA wavefunction, showing that this solution accurately describes the trapped mixture at finite, large but equal interactions.

V. OUTLOOK AND PERSPECTIVES

In this work we have studied the exact solutions of a highly symmetric model for Bose-Fermi mixture in the strongly interacting limit. Our results are relevant for the ongoing experiment on ultracold mixtures of atomic gases in tight atomic waveguides, with particular attention of the case of ^{173}Yb - ^{174}Yb Bose-Fermi mixtures [12] where the fractional mass difference among the two isotopes is small. We have provided first an orthogonal basis set of solutions which span the degenerate manifold. Secondly, we have grouped such solutions on the basis of the Casimir invariant, associated to a given Young tableau. Finally, we have analyzed two special solutions of the problem and discussed their symmetry according to the average value of the Casimir operator. By comparing with DMRG simulations, we have found that the wavefunction obtained by generalizing the Bethe-Ansatz solution to trapped systems accurately describes the density

profile and momentum distribution of the mixture at finite, large but equal BB and BF coupling strengths. This wavefunction can be used to describe the Bose-Fermi mixture in arbitrary external potential. Splittings and mixing of the states with different symmetries are expected when different masses and different BB and BF coupling constants are chosen. Our solution serves as a guideline for further numerical studies. This work opens also the way to the study of the dynamical properties of the strongly interacting Bose-Fermi mixture. Signatures of strong correlations could be found in the collective excitation spectrum. It would also be interesting to investigate how particular states in the degenerate manifold can be prepared and addressed.

ACKNOWLEDGMENTS

We thank F. Deuretzbacher for suggestions on the $N = 3$ case, M. Rizzi for help with the DMRG code and B. Grémaud for discussions. This work has been developed by using the DMRG code released within the "Powder with Power" project (www.qti.sns.it). We acknowledge support from the MIDAS STREP project, the

Handy-Q ERC project and from the CNRS PEPS-PTI "Quantum gases and condensed matter". ChM acknowledges support from the CNRS PICS Grant No. 4159 and from the France-Singapore Merlion program, FermiCold grant No. 2.01.09. Centre for Quantum Technologies is a Research Centre of Excellence funded by the Ministry of Education and the National Research Foundation of Singapore.

Appendix A: Casimir operator on the BBFF basis

For $N_B = 2, N_F = 2$ the representation of the Casimir operator $\mathcal{C} = \sum_{i < j} (ij)$ on the orthonormal BBFF configuration basis reads

$$\begin{pmatrix} 0 & 1 & -1 & 1 & -1 & 0 \\ 1 & 0 & 1 & 1 & 0 & -1 \\ -1 & 1 & 0 & 0 & 1 & -1 \\ 1 & 1 & 0 & 0 & 1 & 1 \\ -1 & 0 & 1 & 1 & 0 & 1 \\ 0 & -1 & -1 & 1 & 1 & 0 \end{pmatrix}. \quad (\text{A1})$$

For $N_B = 3, N_F = 3$ the Casimir operator reads

$$\begin{pmatrix} 0 & 1 & -1 & 1 & 1 & -1 & 1 & 0 & 0 & 0 & 1 & -1 & 1 & 0 & 0 & 0 & 0 & 0 & 0 & 0 \\ 1 & 0 & 1 & -1 & 1 & 0 & 0 & -1 & 1 & 0 & 1 & 0 & 0 & -1 & 1 & 0 & 0 & 0 & 0 & 0 \\ -1 & 1 & 0 & 1 & 0 & 1 & 0 & -1 & 0 & 1 & 0 & 1 & 0 & -1 & 0 & 1 & 0 & 0 & 0 & 0 \\ 1 & -1 & 1 & 0 & 0 & 0 & 1 & 0 & -1 & 1 & 0 & 0 & 1 & 0 & -1 & 1 & 0 & 0 & 0 & 0 \\ 1 & 1 & 0 & 0 & 0 & 1 & -1 & -1 & 0 & 1 & 0 & 0 & 0 & 0 & 0 & 0 & -1 & 1 & 0 & 0 \\ -1 & 0 & 1 & 0 & 1 & 0 & 1 & 1 & 0 & -1 & 0 & 1 & 0 & 0 & 0 & 0 & -1 & 0 & 1 & 0 \\ 1 & 0 & 0 & 1 & -1 & 1 & 0 & 0 & 1 & -1 & 0 & 0 & 1 & 0 & 0 & 0 & 0 & -1 & 1 & 0 \\ 0 & -1 & -1 & 0 & 1 & 1 & 0 & 0 & 1 & 1 & 0 & 0 & 0 & 1 & 0 & 0 & -1 & 0 & 0 & 1 \\ 0 & 1 & 0 & -1 & -1 & 0 & 1 & 1 & 0 & 1 & 0 & 0 & 0 & 0 & 1 & 0 & 0 & -1 & 0 & 1 \\ 0 & 0 & 1 & 1 & 0 & -1 & -1 & 1 & 1 & 0 & 0 & 0 & 0 & 0 & 0 & 1 & 0 & 0 & -1 & 1 \\ 1 & 1 & 0 & 0 & 1 & 0 & 0 & 0 & 0 & 0 & 0 & 1 & -1 & 1 & -1 & 0 & 1 & -1 & 0 & 0 \\ -1 & 0 & 1 & 0 & 0 & 1 & 0 & 0 & 0 & 0 & 1 & 0 & 1 & 1 & 0 & -1 & 1 & 0 & -1 & 0 \\ 1 & 0 & 0 & 1 & 0 & 0 & 1 & 0 & 0 & 0 & -1 & 1 & 0 & 0 & 1 & -1 & 0 & 1 & -1 & 0 \\ 0 & -1 & -1 & 0 & 0 & 0 & 0 & 1 & 0 & 0 & 1 & 1 & 0 & 0 & 1 & 1 & 1 & 0 & 0 & -1 \\ 0 & 1 & 0 & -1 & 0 & 0 & 0 & 0 & 1 & 0 & -1 & 0 & 1 & 1 & 0 & 1 & 0 & 1 & 0 & -1 \\ 0 & 0 & 1 & 1 & 0 & 0 & 0 & 0 & 0 & 1 & 0 & -1 & -1 & 1 & 1 & 0 & 0 & 0 & 1 & -1 \\ 0 & 0 & 0 & 0 & -1 & -1 & 0 & -1 & 0 & 0 & 1 & 1 & 0 & 1 & 0 & 0 & 0 & 1 & 1 & 1 \\ 0 & 0 & 0 & 0 & 1 & 0 & -1 & 0 & -1 & 0 & -1 & 0 & 1 & 0 & 1 & 0 & 1 & 0 & 1 & 1 \\ 0 & 0 & 0 & 0 & 0 & 1 & 1 & 0 & 0 & -1 & 0 & -1 & -1 & 0 & 0 & 1 & 1 & 1 & 0 & 1 \\ 0 & 0 & 0 & 0 & 0 & 0 & 0 & 1 & 1 & 1 & 0 & 0 & 0 & -1 & -1 & -1 & 1 & 1 & 1 & 0 \end{pmatrix}. \quad (\text{A2})$$

Appendix B: Demonstration of the symmetry of a special wavefunction

We prove here below that for odd $N_B = N_F$ the GM wavefunction has the symmetry of the Y tableau.

This readily follows from the simple expression of the GM wavefunction on the BBFF basis $\Psi_{GM} = \sum_{\alpha=1}^{N! / N_F! / N_B!} \Psi_{\alpha}$, and from the fact that for odd values of N_F and N_B each line of the matrix which represents the

Casimir operator on the BBFF basis has $N_B N_F$ non-vanishing entries with value 1 in $N_B(N_F + 1)/2$ cases and value -1 in $N_B(N_F - 1)/2$ cases. Each line of the matrix corresponds then equally to the value of the average of the Casimir operator, $\langle \mathcal{C} \rangle = \langle \Psi | \mathcal{C} | \Psi \rangle / \langle \Psi | \Psi \rangle$,

and its value corresponds to the maximal eigenvalue $\mathcal{C}_Y = N_B = N_F$. For other values of N_B, N_F the representation of the Casimir operator is more complicated to predict and the above demonstration does not hold.

-
- [1] B. Paredes *et al.*, Nature **429**, 277 (2004).
 [2] T. Kinoshita, T. R. Wenger, and D. S. Weiss, Science **305**, 5687 (2004).
 [3] T. Kinoshita, T. R. Wenger, and D. S. Weiss, Nature **440**, 900 (2006).
 [4] S. Palzer, C. Zipkes, C. Sias, and M. Köhl, Phys. Rev. Lett. **103**, 150601 (2009).
 [5] A. van Amerongen *et al.*, Phys. Rev. Lett **100**, 090402 (2008).
 [6] M. D. Girardeau, J. Math. Phys. **1**, 516 (1960).
 [7] F. Schreck *et al.*, Phys. Rev. Lett. **87**, 080403 (2001).
 [8] A. G. Truscott *et al.*, Science **291**, 2570 (2001).
 [9] Z. Hadzibabic *et al.*, Phys. Rev. Lett. **88**, 160401 (2002).
 [10] C. Silber *et al.*, Phys. Rev. Lett. **95**, 170408 (2005).
 [11] S. Ospelkaus *et al.*, Phys. Rev. Lett. **97**, 120403 (2006).
 [12] T. Fukuhara, S. Sugawa, Y. Takasu, and Y. Takahashi, Phys. Rev. A **79**, 021601 (2009).
 [13] K. K. Das, Phys. Rev. Lett. **90**, 170403 (2003).
 [14] M. A. Cazalilla and A. F. Ho, Phys. Rev. Lett. **91**, 150403 (2003).
 [15] C. K. Lai and C. N. Yang, Phys. Rev. A **3**, 393 (1971).
 [16] M. T. Batchelor, M. Bortz, X. W. Guan, and N. Oelkers, Phys. Rev. A **72**, 061603 (2005).
 [17] A. Imambekov and E. Demler, Phys. Rev. A **73**, 021602 (2006).
 [18] H. Frahm and G. Palacios, Phys. Rev. A **72**, 061604 (2005).
 [19] A. Imambekov and E. Demler, Ann. Phys. **321**, 2390 (2006).
 [20] Xiangguo Yin, Shu Chen, and Yunbo Zhang, Phys. Rev. A **79**, 053604 (2009).
 [21] M. D. Girardeau and A. Minguzzi, Phys. Rev. Lett. **99**, 230402 (2007).
 [22] B. Y. Fang, P. Vignolo, C. Miniatura, and A. Minguzzi, Phys. Rev. A **79**, 023623 (2009).
 [23] K. Lelas, D. Jukić, and H. Buljan, Phys. Rev. A **80**, 053617 (2009).
 [24] Xiaolong Lü, Xiangguo Yin, Yunbo Zhang, Phys. Rev. A **81**, 043607 (2010).
 [25] F. Deuretzbacher *et al.*, Phys. Rev. Lett. **100**, 160405 (2008).
 [26] Liming Guan, Shu Chen, Yupeng Wang, and Zhong-Qi Ma, Phys. Rev. Lett. **102**, 160402 (2009).
 [27] M. Hamermesh, *Group theory and its applications to physical problems* (Dover, New York, 1989).
 [28] A. Novoselsky and J. Katriel, Phys. Rev. A **49**, 833 (1994).
 [29] C. N. Yang, Chinese Physics Letters **26**, 120504 (2009).
 [30] C. N. Yang, Phys. Rev. Lett. **19**, 1312 (1967).
 [31] B. Sutherland, Phys. Rev. Lett. **20**, 98 (1968).
 [32] Ya-Jiang Hao, Chin. Phys. Lett. **28**, 010302 (2011).
 [33] S. Zöllner, H.-D. Meyer and P. Schmelcher, Phys. Rev. A **78**, 013629 (2008).
 [34] Note that in the homogeneous limit the GM wavefunction does not coincide with the Bethe-Ansatz solution at strong coupling.
 [35] M. Ogata and H. Shiba, Phys. Rev. B **41**, 2326 (1990)
 [36] An open source version of the code is available at <http://www.qti.sns.it/dmrg/phome.html>